Journal of Non-Crystalline Solids 354 (2008) 5444–5452

Contents lists available at ScienceDirect

Journal of Non-Crystalline Solids

journal homepage: www.elsevier.com/locate/jnoncrysol

Investigation on heat transfer performance of fluoride-free and titanium-bearing mold fluxes

Xin Qi *, Guang-Hua Wen, Ping Tang

College of Materials Science and Engineering, Chongqing University, 174, Shazhengjie, Chongqing 400044, China

ARTICLE INFO

Article history:
Received 3 March 2008
Received in revised form 13 August 2008
Available online 18 October 2008

PACS:
61.43.F
61.43
66.20
44.10

Keyword:
Slags

ABSTRACT

Fluorine erodes continuous casters and pollutes the environment. In order to reduce the damage caused by fluorine, it is necessary and urgent to carry out research on fluoride-free mold fluxes. There has been little research done on the heat transfer performance of fluoride-free mold fluxes either domestically or abroad. The present work adopted TiO_2 to take the place of fluorine in mold fluxes and studies its heat transfer performance. Heat flux simulation equipment was developed and the heat flux density of titanium-bearing mold fluxes containing TiO_2 was measured; in addition, a solid slag film was obtained. The crystallization behavior and the change of activation energy for crystallization of the slag film was analyzed. Our results show that when the TiO_2 content is increased, the heat flux density of fluoride-free mold fluxes decreases, the crystallization activation energy of mold fluxes is diminished and the crystallization ratio of mold fluxes increases, and the mineral phase of the slag film turns from akermanite into perovskite. When the basicity is increased, the heat flux of fluoride-free mold fluxes is reduced, the crystallization ratio of mold fluxes increases and the mineral phase of the slag film turns from unitary akermanite into the coexistence of two phases of akermanite and perovskite. Furthermore, the capability of fluoride-free and titanium-bearing mold fluxes to control heat transfer is better, so it can be expected to replace industrial slag containing fluorine completely.

1. Introduction

In the continuous casting process, mold fluxes have an important influence on the surface quality of continuous casting slab. Generally, the basic composition of mold fluxes is $CaO–SiO_2–Al_2O_3–Na_2O–CaF_2$ [1–3], in which fluoride mainly controls the viscosity, solidification temperature, and crystallization behavior of mold flux films. These characteristics directly influence the lubrication and heat transfer of a mold flux film. However, in the course of its use, the volatilization and acidification of fluoride poses a significant health hazard, causes environmental pollution and intensifies the erosion to continuous caster [4]. As a result, developing fluoride-free continuous casting mold fluxes is of great significance.

At present, the research on fluoride-free mold fluxes is mainly concentrated on improving the melting behavior and viscosity characteristics of fluoride-free mold fluxes, as well as on increasing the evenness and stability of melting[5,6]. However, research on how to effectively control the heat flux of fluoride-free mold fluxes is less widespread. The research of Tylor et al. [7] shows that increasing the crystallization ratio of solid mold flux film can decrease the heat flux and thermal gradient through the mold and is conducive to reducing longitudinal cracks of the slab. In industrial slag containing fluorine, heat transfer is usually controlled by precipitating cuspidine ($3CaO \cdot 2SiO_2 \cdot CaF_2$). Since fluoride-free mold fluxes contain no fluorine, there exists another crystal to control the transfer of heat.

Wen et al. [8,9] and Hideko et al. [10] found that adding TiO_2 to mold fluxes easily generated a crystal with a high melting point which can replace the cuspidine generated by fluorine in mold fluxes to control heat transfer. They also carried out research on the incubation time, melting point, viscosity and heat transfer of crystallization and on aspects of production and application, but without further discussion of the heat transfer mechanism. In this work, a homebuilt apparatus was used to examine the influence of the TiO_2 content and basicity in fluoride-free mold fluxes on the heat transfer performance and crystallization behavior of the slag film.

2. Experimental method

2.1. Preparation of mold fluxes

The TiO_2 content ranged from 1% to 10% and the value of $R\left(=\frac{CaO}{SiO_2}\text{, dual basicity}\right)$ ranged from 0.6 to 1.2. In order to ensure

* Corresponding author. Tel.: +86 023 65105202; fax: +86 023 65105202.
E-mail address: qixin@cqu.edu.cn (X. Qi).

0022-3093/$ - see front matter © 2008 Elsevier B.V. All rights reserved.
doi:10.1016/j.jnoncrysol.2008.09.012

that the slag had the appropriate viscosity and melting point, a particular amount of fusing agent, such as B_2O_3, Li_2O, Na_2O, MgO and MnO, was added into the slag. The melting point of each type of slag was measured with the hemisphere-point method and the viscosity was measured with a rotary viscometer. The chemical composition, measured melting point T_M and viscosity η below 1300 °C of various fluoride-free mold fluxes are listed in Table 1. In addition, three industrial mold fluxes, 3D, 2CK and M16 containing fluorine used in medium carbon steel and peritectic steel continuous casting were measured. Their melting points T_M and viscosity η at 1300 °C are also listed in Table 1.

2.2. Experimental set-up and method of slag film heat transfer

An apparatus based on the copper finger [9,11] was constructed. Fig. 1 shows the apparatus. Not only was the solid slag film increased, but the temperature difference between water entering and exiting the copper probe was measured, allowing calculation of the heat flux density passing through the slag film. The size of the copper finger was 20 mm × 25 mm × 35 mm. In order to ensure that the flow of cooling water per unit area is similar to that in the real mold, the flow of cooling water is maintained at 300 L/h. The experimental procedure is as follows. First, we put 350 g of prepared slag in a graphite crucible and heat it with a $MoSi_2$ furnace. The temperature was increased to 1400 °C and maintained for about 10 min so that the mold fluxes were completely melted. Then, the water-cooled copper finger (simulating the mold) was immersed into the liquid mold fluxes, taking the point at which the copper finger was completely immerged in the mold fluxes as the starting time $t = 0$ of the experiment. After a period of time, we took the copper finger out of the liquid mold fluxes and obtained the slag film that was adhered to the copper finger. The heat flux density can be defined by the equation [12]:

$$\phi = W \cdot C\Delta T/(F \cdot 1000). \quad (1)$$

In this formula, ϕ is the heat flux density of the film (MW m^{-2}), W refers to the flow of the probe cooling water (kg s^{-1}), ΔT indicates the temperature difference of the water at outlet ($T_B - T_A$) (°C), F represents the effective heat transfer area of the probe (m^2) and C is the specific heat of water (kJ (kg °C)$^{-1}$).

The slag films at three different immersion times are studied. The three immersion times were 10, 20 and 70 s, corresponding to the primary formation stage, intermediate stage and stable stage of the solid slag film based on the theory of unsteady heat transfer [12]. After the solid slag film was obtained, its cross-section was observed by scanning electron microscopy and the mineral phase was analyzed. Some of the slag film was crushed to a grain size of 400 mesh and its crystallization ratio was measured with an X-ray diffractometer (XRD). Glass from another part of the slag film was removed with carborundum paper and the phase of the remaining crystal slag film was analyzed with an XRD.

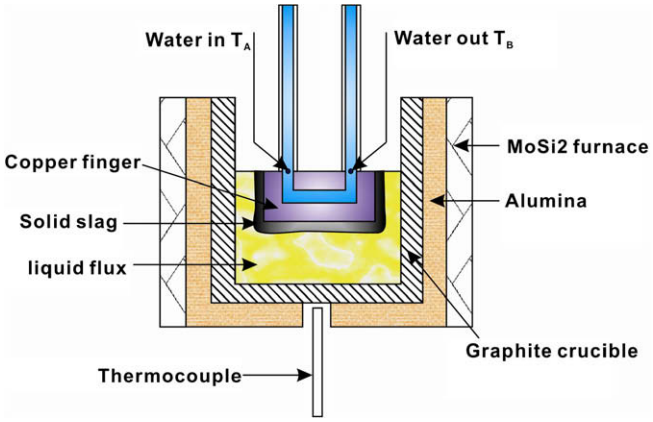

Fig. 1. The HF-200 heat flux simulator set-up of mold slag film.

In this work, we used a Ricoh D/MAX-IIIC X-ray diffractometer and scanning electron microscope to analyze the slag film formed at different immersion times and studied their crystallization ratio and mineral phases.

2.3. Measurement of activation energy for crystallization

Crystal nucleation and growth in the glass are mainly dependent on the activation energy E needed for the glass to cross the boundary surface and enter the crystalline phase. At the same time, the activation energy value E of crystallization is also a measure of the inhibition to crystallization. This energy can be calculated using the formula of Kissinger [16,17].

Kissinger found that the crystallization volume fraction as a function of time is fundamental to the non-isothermal method and is given by

$$\frac{dx}{dt} = A(1-x)e^{-\frac{E}{RT}}. \quad (2)$$

When the reaction rate is at a maximum, its derivative with respect to time is zero. Solving Eq. (2) for $(d/dt)(dx/dt)$ yields

$$\frac{d}{dt}\left(\frac{dx}{dt}\right) = \frac{dx}{dt}\left(\frac{E}{RT^2}\cdot\frac{dT}{dt} - Ae^{-\frac{E}{RT}}\right). \quad (3)$$

The maximum value of dx/dt occurs at temperature T_p, defined by

$$Ae^{-\frac{E}{RT_p}} = \frac{E}{RT_p^2}\frac{dT}{dt}. \quad (4)$$

This is the equation derived by Murray and White [19].

Table 1
The chemical compositions (in mass%) and physical properties of the studied slags

Number	Composition											$R\left(\frac{CaO}{SiO_2}\right)$	T_M (°C)	η (Pa s at 1573 K)
	CaO	Al_2O_3	SiO_2	MgO	B_2O_3	Na_2O	Li_2O	MnO	TiO_2	FeO	CaF_2			
1	38.9	0.7	38.9	4.5	4.5	5.5	1.2	4.5	1.1	0.2	0	1.0	1090	0.345
2	36.8	2.1	36.8	4.5	4.5	5.5	1.2	4.5	3.4	0.7	0	1.0	1105	0.417
3	34.9	3.3	34.9	4.5	4.5	5.5	1.2	4.5	5.6	1.1	0	1.0	1122	0.346
4	34.0	3.9	34.0	4.5	4.5	5.5	1.2	4.5	6.7	1.3	0	1.0	1126	0.324
5	33.0	4.5	33.0	4.5	4.5	5.5	1.2	4.5	7.8	1.5	0	1.0	1132	0.399
6	31.1	5.8	31.1	4.5	4.5	5.5	1.2	4.5	9.9	1.9	0	1.0	1119	0.509
7	25.5	3.8	42.5	4.5	4.5	5.5	1.2	4.5	6.7	1.3	0	0.6	1048	0.884
8	30.2	3.9	37.7	4.5	4.5	5.5	1.2	4.5	6.7	1.3	0	0.8	1088	0.418
9	32.2	3.8	35.8	4.5	4.5	5.5	1.2	4.5	6.7	1.3	0	0.9	1095	0.442
10	37.0	3.9	30.9	4.5	4.5	5.5	1.2	4.5	6.7	1.3	0	1.2	1119	0.270
3D	41.0	5.1	31.7	1.6	0	9.1	0	0	0	2.0	9.5	1.3	1065	0.131
2CK	40.9	4.5	34.0	0	0	11.0	0	0	0	0	9.6	1.2	1100	0.116
M16	35.3	4.4	35.7	0	0	9.7	1.4	0	0	0	13.5	1.0	1086	0.120